Featured Article

Gene Expression Profiles Predict Survival and Progression of Pleural Mesothelioma

Harvey I. Pass,[1] Zhandong Liu,[2] Anil Wali,[1] Raphael Bueno,[6] Susan Land,[3] Daniel Lott,[3] Fauzia Siddiq,[1] Fulvio Lonardo,[4] Michele Carbone,[5] and Sorin Draghici[2]

[1]Thoracic Oncology, Karmanos Cancer Institute, [2]Department of Computer Science, and [3]Center for Molecular Medicine and Genetics, Wayne State University, Detroit, Michigan; [4]Department of Pathology, Harper University Hospital, Detroit, Michigan; [5]Department of Pathology, Cardinal Bernardin Cancer Center, Loyola University, Maywood, Illinois; and [6]Division of Thoracic Surgery, Brigham and Women's Hospital, Harvard Medical School, Boston, Massachusetts

Abstract

Purpose: **Clinical outcomes for malignant pleural mesothelioma (MPM) patients having surgery are imprecisely predicted by histopathology and intraoperative staging. We hypothesized that gene expression profiles could predict time to progression and survival in surgically cytoreduced pleural mesothelioma of all stages.**

Experimental Design: **Gene expression analyses from 21 MPM patients having cytoreductions and identical postoperative adjuvant therapy were performed using the U95 Affymetrix gene chip. Using both dChip and SAM, neural networks constructed a common 27 gene classifier, which was associated with either the high-risk and low-risk group of patients. Data were validated using real-time PCR and immunohistochemical staining. The 27 gene classifier was also used for validation in a separate set of 17 MPM patients from another institution.**

Results: **The groups predicted by the gene classifier recapitulated the actual time to progression and survival of the test set with 95.2% accuracy using 10-fold cross-validation. Clinical outcomes were independent of histology, and heterogeneity of progression and survival in early stage patients was defined by the classifier. The gene classifier had a 76% accuracy in the separate validation set of MPMs.**

Conclusions: **These data suggest that pretherapy gene expression analysis of mesothelioma biopsies may predict which patients may benefit from a surgical approach.**

Received 4/21/03; revised 10/12/03; accepted 10/14/03.

Grant support: Early Detection Research Network, National Cancer Institute/NIH U01 CA 084986, by Merit Review Funding from the Department of Veterans Affairs, and by a grant from the Mesothelioma Applied Research Foundation (R. B.).

The costs of publication of this article were defrayed in part by the payment of page charges. This article must therefore be hereby marked *advertisement* in accordance with 18 U.S.C. Section 1734 solely to indicate this fact.

Requests for reprints: Harvey I. Pass, Harper University Hospital, 3990 John R, Suite 2102, Detroit, MI 48201. Phone: (313) 745-8746; Fax: (313) 993-0572; E-mail: hpass@dmc.org.

Introduction

Malignant pleural mesothelioma (MPM) is an orphan disease of which the management has defied curative options (1). The incidence of MPM worldwide is increasing, and the estimated number of deaths over the next 30 years from MPM in Western Europe alone could approach 250,000 (2). Our understanding of the pathophysiology of the disease, however, has improved with the advent of molecular investigations of the downstream effects of asbestos (3), as well as the realization that SV40 is linked with the disease in >60% of the cases (4). Studies of the molecular genetics of the disease have revealed the importance of signal transduction pathways including the epidermal growth factor receptor (5) and activator protein (6), as well as asbestos-SV40 interactions, which could explain such phenomena as increased angiogenesis (7), telomerase (8, 9), MET overexpression (10, 11), abrogation of p53-induced apoptosis (12), and abnormalities of immune surveillance (13) among other findings.

There have been few global investigations using gene array technologies of the multiple genetic events in MPM due to the lack of uniformly treated patients with carefully documented survival and recurrence data, and the absence of large archives of banked frozen tissue with adequately preserved RNA. In addition to the gene-based classification (14), the ability to prognosticate on the basis of gene expression data from biopsy harvests could have important therapeutic implications for this group of unfortunate patients. Our hypothesis is that gene arrays performed on operative specimens from uniformly treated mesothelioma patients could predict survival and time to progression, and could cluster groups of patients as good or poor risk. Our test set population included stages I-III MPM patients resected by one surgeon. We analyzed our gene expression data using two programs, significance analysis microarrays (SAM) and dCHIP, to see whether concordant genes from both analyses could correctly cluster the patients into good or poor risk cohorts.

Materials and Methods

Patient Population. Tumor and normal tissues from 21 patients with MPM treated at the National Cancer Institute and the Karmanos Cancer Institute between August 1993 and May 2001 were used as the test set for the studies described below. Consent was received and the project approved by the local Institutional Review Boards. All of the patients had cytoreductive surgery, mediastinal lymph node dissection with staging by the International Mesothelioma Interest Group staging system (15), followed by postoperative cisplatinum-based chemotherapy. All of the patients were followed from the surgery until death or through February 2003 with computerized tomography of the chest every 3 months. Interval change, which suggested progression of the MPM, was documented whenever possible by histological confirmation of disease. Tumors were classified as having epithelial, sarcomatoid, or mixed histology MPM by two

of the authors (F. L. and M. C.). All of the tumor specimens contained a tumor cellularity of >85%.

Gene Expression Profiling. RNA isolation and cRNA synthesis were performed as described (16). Each probe array was scanned twice (Hewlett-Packard GeneArray Scanner), the images overlayed, and the average intensities of each probe cell compiled. dChip and SAM were used for expression profiling.

Real-Time Quantitative Reverse Transcription-PCR. Real-time quantitative reverse transcription-PCR was used to confirm differential gene expression profile of Plasmolipin, Calumenin, and IGFBP5. cDNAs were synthesized from 3 μg total RNA using an oligodeoxythymidylic acid primer and the Superscript II reverse transcription kit (Life Technologies, Inc.). The primers used were: Plasmolipin sense, 5′-ATGTTC-GTCGCTGTCTTCCT-3′; antisense, 5′-ATCATCACCAAAC-ACGCAAA-3′; Calumenin sense, 5′-CGCTGGATTTACGAG-GATGT-3′; antisense 5′-GCAGGAAAGCTGTGAACTCC-3′; IGFBP5 sense 5′-GAGCTGAAGGCTGAAGCAGT-3′, antisense 5′-GAATCCTTTGCGGTCACAAT-3′.

The amplified PCR products were 248 bp Plasmolipin fragment, a 235 bp Calumenin fragment, and a 237 bp IGFBP5 fragment. Reactions containing 1 μg cDNA, SYBR green sequence detection reagent, and sense and antisense primers were assayed on an ABI 7700 sequence detection system (Applied Biosystems). The PCR conditions were one cycle at 50°C for 2 min, one cycle at 95°C for 10 min, and 40 cycles of 95°C for 15 s, 60°C for 1 min. The accumulation of PCR product was measured in real time as the increase in SYBR green fluorescence, and the data were analyzed using the Sequence Detector program v1.6.3 (Applied Biosystems). Standard curves relating initial template copy number to fluorescence and amplification cycle were generated using the amplified PCR product as a template and were used to calculate gene concentration (normalized to β-actin values) in nM/μg cDNA.

Immunohistochemical Staining. Deparaffinized sections were stained manually, using the avidin-biotin complex technique. In brief, 4 μm sections were collected on gelatin-coated slides, deparaffinized, and rehydrated via passage through graded alcohol solutions, according to standard histological techniques. Heat-induced epitope retrieval was obtained by heating slides for 20′ in a citrate buffer (2 mM citric acid/10 mM Na citrate; pH 6) in a steam bath, followed by cooling down for 20′ at room temperature. Slides were presaturated with 0.05% BSA in PBS for 10′, quenched in 2% H_2O_2 for 10′, and preincubated with 0.5% nonimmune goat serum (Sigma) for 10′ at room temperature. The sections were then incubated with the primary antibodies. Antibodies used, dilutions, and incubation conditions were monoclonal Nm 23 antibody (Santa Cruz Biotechnology-H1; sc 465) 1:20 dilution, overnight incubation at 4°C; monoclonal Integrin α 6 (Santa Cruz Biotechnology BQ; sc-13542) 1:10 dilution, overnight incubation at 4°C; and polyclonal FGF-7 (Santa Cruz Biotechnology-C19; sc-1365), 1:40 dilution, 2-h incubation at room temperature. After three washes in BSA/PBS (5′ each) localization of the primary antibody and color development were obtained by incubation with biotinylated antimouse (monoclonal antibodies) or antigoat (FGF-7) secondary antibodies (Vector), followed by incubation with streptavidin-coupled horseradish peroxidase, using an avidin-biotin detection kit, with AEC as the chromogen (Vector Labs, Burlingame, CA). Sections were lightly counterstained with hematoxylin (Sigma) and coverslipped. Positive controls were included with each run and included colon cancer for Nm23, normal skin for Integrin α 6, and ductal carcinoma of breast for FGF-7. Negative controls were included with each run by omitting the primary antibody. Score was separately assessed for intensity and extent of positivity. Intensity was scored on a scale of 1 (lightest) to 3 (strongest). The extent of tumor cells positivity was scored as negative, no stain; focal, ≤10% positive tumor cells; moderate, ≥10% positive cells ≤50%; and diffuse, ≥50% positive tumor cells. Positive stain occurred in the cytoplasm.

Table 1 Mesothelioma test set characteristics

Survivor group	Number	Sex	IMIG Stage	Histology	Survival (mos.)	Status	Time to recurrence	Progression
Short-term	1	M	III	Epithelial	2	D	1.0	Y
	2	M	II	Epithelial	3.6	D	1.8	Y
	3	M	III	Epithelial	5.2	D	3.4	Y
	8	M	III	Epithelial	3.2	D	3.2	Y
	12	M	III	Biphasic	4.3	D	3.0	Y
	17	M	III	Epithelial	4.8	D	1.64	Y
	39	M	II	Biphasic	2	D	1.5	Y
	38	M	III	Biphasic	2	D	1.75	Y
	30	F	III	Epithelial	7.3	D	2.2	Y
	29	M	III	Biphasic	1.7	D	1.3	Y
	33	M	II	Epithelial	10	D	8	Y
Long-term	4	M	III	Epithelial	48	A	17	Y
	5	M	I	Epithelial	95	A	95	N
	6	F	III	Biphasic	25	D	22	Y
	7	M	III	Biphasic	32	D	14	Y
	11	M	I	Epithelial	95	A	14	Y
	16	M	II	Epithelial	99	A	15	Y
	19	F	III	Sarcomatoid	103	A	6	Y
	21	F	I	Epithelial	102	A	60	Y
	22	F	III	Epithelial	28	D	12	Y
	15	M	II	Epithelial	58	D	12	Y

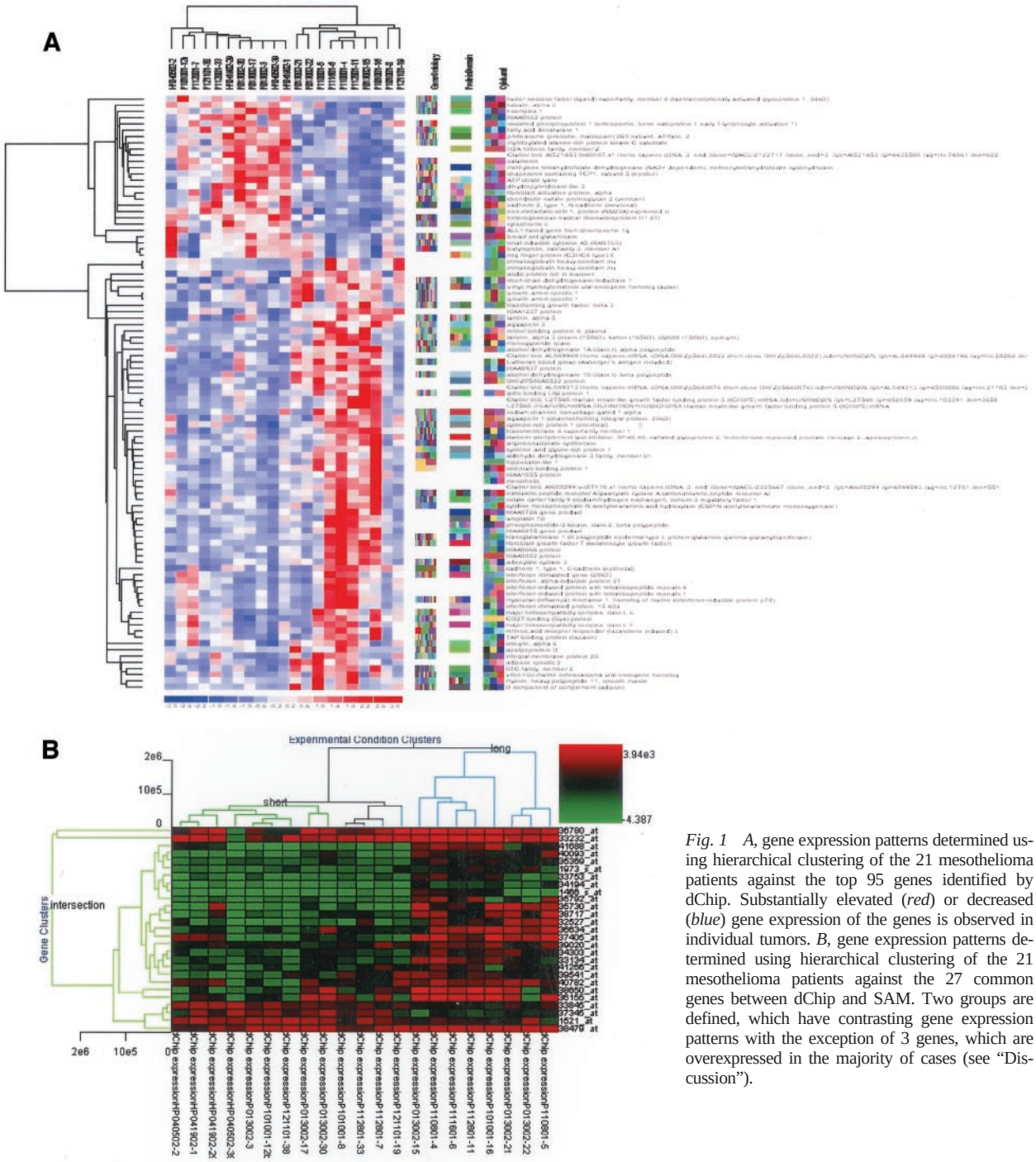

Fig. 1 *A*, gene expression patterns determined using hierarchical clustering of the 21 mesothelioma patients against the top 95 genes identified by dChip. Substantially elevated (*red*) or decreased (*blue*) gene expression of the genes is observed in individual tumors. *B*, gene expression patterns determined using hierarchical clustering of the 21 mesothelioma patients against the 27 common genes between dChip and SAM. Two groups are defined, which have contrasting gene expression patterns with the exception of 3 genes, which are overexpressed in the majority of cases (see "Discussion").

Data Analysis and Neural Network Methods. *T* tests were used to identify differences in mean gene expression levels between comparison groups. We constructed of the classifiers using a multilayer feedforward backpropagation neural network. A three layer feed forward artificial neural network was trained based on the expression value of differentially regulated genes, and the accuracy of the neural network was confirmed with 10-fold cross-validation. The 10-fold cross-validation involves constructing 10 different classifiers in 10 training runs. Each training run divides the available data into a training set, including 90% of the data and a validation set including 10% of the data. The classifier is constructed based on the training set and tested on the validation set. Each training run leaves out different patterns such as at the end of the entire process, each

Table 2 Confusion matrix results for the test set and validation set

	Classified by the 27 gene expression array as	
	Good risk	Poor risk
Wayne/KCI test set "true class"		
Long	9	1
Short	0	11
B&W validation set "true class"		
Long	5	3
Short	1	8

available patient will have been left out at least once. The performance reported represents an average of these 10 training runs. The process ensures that the resulting classifiers are always tested on data that has never been used during the training, thus testing its generalization abilities. We calculated the intersection of the genes selected by the dChip and Sam, and constructed a similar neural network classifier based on only those genes that were selected by both methods. To inspect visually the expression profiles of the genes, a hierarchical clustering was constructed for each group of genes using average linkage and standardized Euclidean distance.

The performance of each classifier was assessed in two ways. Firstly, each classifier was tested and assessed using 10-fold cross-validation, as described above. Secondly, we used the trained classifier on a previously unseen data set of 17 mesothelioma patients including 8 long-term survivors and 9 short-term survivors. These data were obtained from the Division of Thoracic Surgery of the Brigham and Women's Hospital (16). Kaplan Meier survival plots and log rank tests were used to assess differences between poor and good risk groups using MedCalc Software (Mariakerke, Belgium).

Onto-Express (OE) Analysis. Using OE (17), we performed a functional analysis to identify the main biological processes and pathways involving these prognostic genes. OE is a tool designed to mine the available functional annotation data and find relevant biological processes. The input to OE is the list of GenBank accession numbers, Affymetrix probe IDs, or UniGene cluster IDs. OE constructs a functional profile for each of the Gene Ontology categories (18), including cellular component, biological process, and molecular function, as well as biochemical function and cellular role, as defined by Proteome. As biological processes can be regulated within a local chromosomal region (*e.g.*, imprinting), an additional profile is constructed for the chromosome location. Statistical significance values are calculated for each category using either a hypergeometric or binomial distribution depending on the number of genes on the array used.

Results

Hierarchical Profile Clustering Yields Two Mesothelioma Subsets. Using the U95 Affymetrix oligonucleotide arrays, we generated profiles for 21 MPMs, which had been defined as "short-term" and "long-term" groups based on their actual survival from operation as either $<$ or $>$12 months (Table 1). Median survival time for the short-term group was 3.6 months (range, 2–10 months) compared with 58 months (range, 25–102 months) for the long-term group ($P < 0.0001$). The time from surgery to radiographic progression of disease was a median of 1.8 months (range, 1–8 months) and 14.5 months (range, 6–95 months) for the short- and long-term groups, respectively ($P < 0.0001$).

Selection of Differentially Regulated Genes: dChip. The dChip software package (19) normalized the 21 Affymetrix chips by the chip with median expression value. The unsupervised clustering on all 12,625 of the genes produced a dendogram in which the gene expression profiles of the long- and short-term survivors were not consistently different. A PM/MM model-based normalization was performed to select the genes that were differentially regulated between the long- and short-

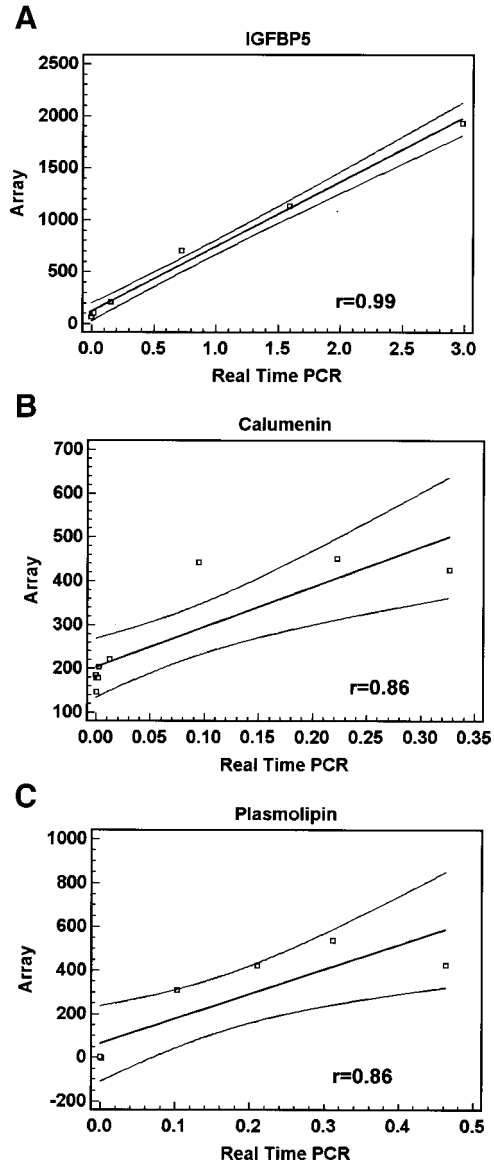

Fig. 2 Validation of gene chip data with real-time PCR for IGFB5, plasmolipin, and calumenin. The same sample RNA for the array analyses were used for the real-time PCR. (See text for details).

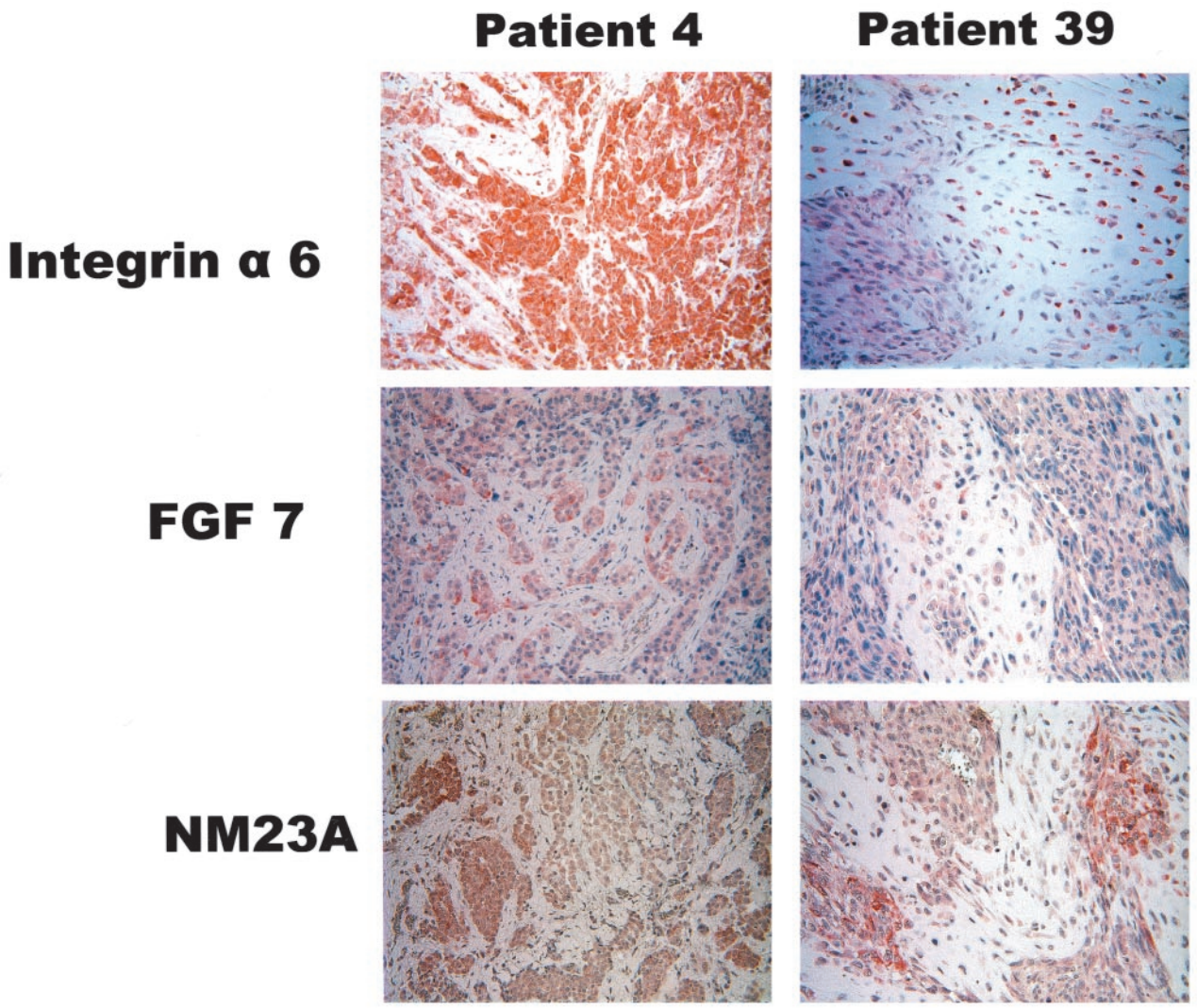

Fig. 3 Immunohistochemical analysis of integrin α-6, FGF07, and NM23A comparing 1 patient from each of the two clusters. Tumor staining was more prominent in patient 4 compared with patient 39 for integrin and FGF-7 with comparable expression of NM23 in both patients. Magnification, ×40.

term survivor groups with the following criteria: (*a*) E-B > 100; (*b*) E/B > = 1.2 or B/E > = 1.2; and (*c*) two group *t* test has a $P < 0.05$. E and B stand for the average expression value in the experiment (long-term survivors, good risk) and control (short-term survivors, poor risk) groups, respectively. Ninety-five genes satisfied the two criteria above (Fig. 1*A*). These 95 genes were used to construct an artificial neural network with a 95–14-2 architecture. This network achieved an accuracy of 90.5% measured by 10-fold cross-validation. The sensitivity and specificity of this artificial neural network classifier were 90% and 90.9%, respectively.

Selection of Differentially Regulated Genes: SAM. We analyzed the same data using the Significance Analysis of Microarray (20) using a fold change of 1.2 and a delta value of 0.6679. Because of the sensitivity of setting parameters in SAM, we could only select 100 genes (as opposed to 95 in dChip) with a false discovery rate of 26.6%. A neural network constructed a classifier based on these SAM-selected genes with an accuracy of 100% (achieved on 10-fold cross-validation). The sensitivity and specificity of this artificial neural network classifier were 100% and 100%, respectively.

Common Genes between dChip and SAM. To define which important genes were common to dChip and SAM, an unpaired two group comparison was performed on the dChip normalized data. Interestingly, the intersection of the 95 genes selected by dChip with the 100 genes selected by SAM yielded only 27 common genes. This suggested that: (*a*) the data were rather noisy and the subset of good predictors might be <95 genes, and (*b*) at least one but possibly both methods picked up a number of genes that were less than ideal predictors. To investigate these hypotheses, we built a classifier based on the genes common between the two sets (*i.e.*, 95 dChip genes and

Table 3 The 27 common dChip and SAM genes for malignant pleural mesothelioma prognostication

Gene name	Chromosomal location	Probe set	*P*	Average expression	Biologic process
Clusterin (complement lysis inhibitor, SP-40, apolipoprotein J)	8p21-p12	36780_at	0.0014	1158	Lipid metabolism
Transmembrane 4 superfamily member 11 (plasmolipin)	16q13	41688_at	0.0022	206	Myelin distribution
Cysteine-rich protein 1 (intestinal)	7q11.23	33232_at	0.0004	995	Extracellular matrix control
Dishevelled associated activator of morphogenesis 1	14q22.3	33753_at	0.0024	141	Undefined
Homo sapiens mRNA; cDNA DKFZp564B076 (from clone DKFZp564B076)	Ch. 6	34194_at	0.0004	79	Undefined
Alcohol dehydrogenase IB (class I), β polypeptide	4q21-q23	35730_at	0.0056	269	Catalyzes oxidation of alcohol
Human insulin-like growth factor binding protein 5 (IGFBP5)	Ch. 2	38650_at	0.0045	543	Control of cancer proliferation
mRNA	12q11	38717_at	0.0021	266	Undefined
DKFZP586A0522 protein	14q32.33	39020_at	0.0025	322	GO induction and receptor signaling
CD27-binding (Siva) protein	19q13.2	40093_at	0.0051	169	Cell adhesion
Lutheran blood group (Auberger b antigen included)	1p36.1	40782_at	0.0067	354	Nucleotide binding
Short-chain dehydrogenase/reductase 1	5q35.3	33845_at	0.0004	376	Transcription and translation regulation
Heterogeneous nuclear ribonucleoprotein H1 (H)	Ch. 10	34303_at	0.0032	235	Undefined
Homo sapiens, similar to Y43E12A.2.p, clone MGC:33537	11q12.3	35369_at	0.0052	190	Undefined
IMAGE:4821347	3q21.3	35792_at	0.0045	171	Lipid metabolism
KIAA0937 protein	10pter-q25.3	36155_at	0.0036	637	Undefined
Monoglyceride lipase	1q32	36634_at	0.0025	370	DNA repair, cell cycle regulation
KIAA0275 gene product	7q32	37345_at	0.0006	324	Transformation, amyloid formation
BTG family, member 2	1q21-q22	37405_at	0.0044	440	Proliferation, transformation
Calumenin	9q22.32	38749_at	0.0013	630	Oncogenesis
Selenium binding protein 1	3q21.3	39541_at	0.0044	262	Undefined
Acidic (leucine-rich) nuclear phosphoprotein 32 family, member B	2q31.1	41266_at	0.0035	230	Cell adhesion
KIAA1237 protein	10q23.32	32527_at	0.0062	218	Lipid metabolism
Integrin, α6	2p24-p22	33134_at	0.0044	254	Cell proliferation
Adipose specific 2	8q24.12-q24.13	1973_at	0.0002	164	Apoptosis
Adenylate cyclase 3	17q21.3	1521_at	0.0003	435	Invasion, metastasis suppression
V-myc myelocytomatosis viral oncogene homolog (avian)	15q15-q21.1	1466_at	0.0034	86	Growth factor, cell proliferation
Nonmetastatic cells 1, protein (NM23A) expressed in					
Fibroblast growth factor 7 (keratinocyte growth factor)					

100 SAM genes as opposed to the most significant 27 in each analysis). The clustering dendogram for these common 27 genes is seen in Fig. 1*B*. This classifier yielded an accuracy of 95.2% on the validation dataset with 10-fold cross-validation. The confusion matrix is shown in Table 2.

Real-Time PCR and Immunohistochemistry Analyses. Six genes of the 27 were arbitrarily selected to verify the microarray expression data. Real-time quantitative reverse transcription-PCR was performed using primers for Plasmolipin, Calumenin, and IGFBP5 on a minimum of 7 tumor samples. As seen in Fig. 2, there was excellent correlation between the array expression data and the real-time PCR, with the best correlation seen for IGFBP5 (0.99); those for plasmolippin and calumenin were 0.86. Immunohistochemical analysis of integrin α-6, fibroblast growth factor, and IGFBP5 was performed for patients 4 and 39, each representing the two clusters to determine whether RNA expression was reflected appropriately by the corresponding proteins in tumors (Fig. 3). When one compares the expression of the proteins by immunohistochemistry with the clustergram (Fig. 1*B*), it is seen that patient 4 with a more favorable prognosis had elevated levels of integrin and FGF7, and both of these proteins were scored as having a stronger and more focal intensity with more cells staining in patient 4 than patient 39. Staining for NM23A revealed approximately equal intensity and quantity of cellular staining.

Biological Processes Impacted by MPM. We used OE (21) to identify the biological processes impacted significantly by the 27 differentially regulated genes found by both analysis approaches (Table 3). These biological processes include cell proliferation ($P = 0.016$), lipid metabolism ($P = 0.001$), positive regulation of cell proliferation ($P = 0.025$), cell-cell signaling ($P = 0.095$), regulation of transcription from Pol II promoter ($P = 0.071$), pathogenesis ($P = 0.010$), cell cycle arrest ($P = 0.003$), negative regulation of cell proliferation ($P =$

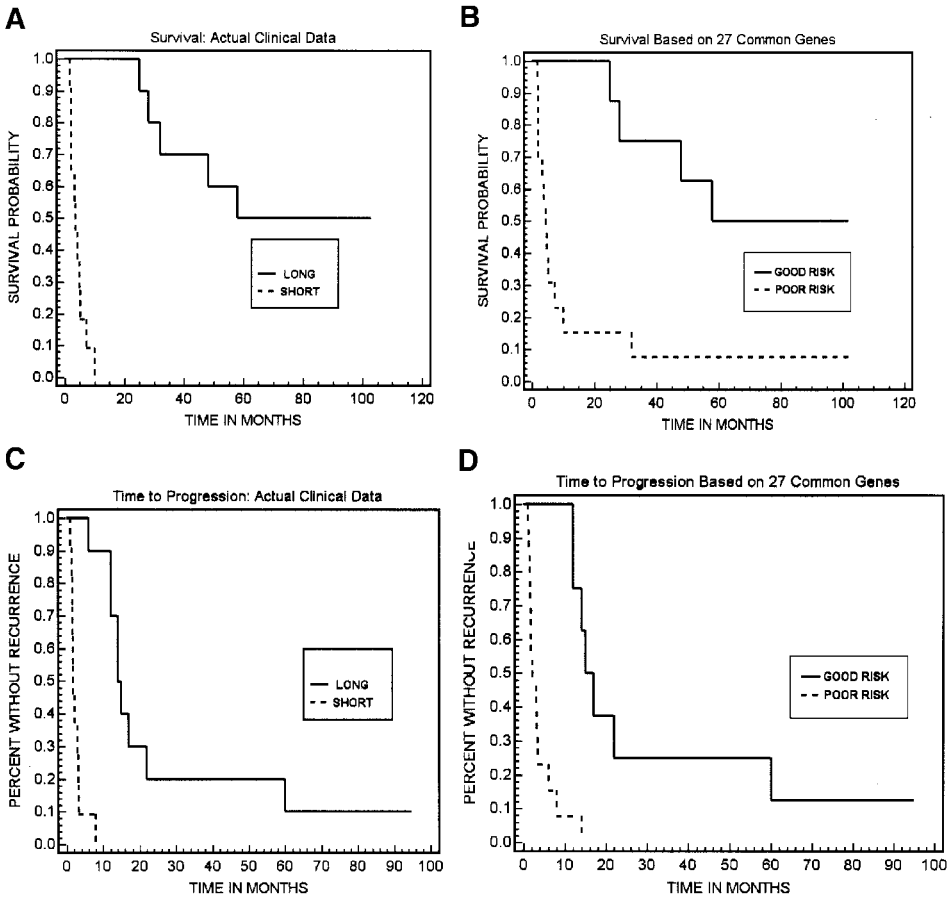

Fig. 4 Survival of the short-term and long-term survival groups as defined in Table 1 were significantly different ($P < 0.0001$). *A* and *B*, survival in the 21 test mesotheliomas based on the 27 gene risk classifier. The poor-risk and good-risk groups differ significantly ($P = 0.0018$), but there is no difference between the gene predicted good-risk group and the actual long-term survivors ($P = 0.6441$), or between the gene predicted poor-risk group and the actual short-term survivors ($P = 0.3226$); *C*, time to progression of the short-term and long-term survival groups as defined in Table 1 was significantly different ($P < 0.0001$). *D*, time to progression in the 21 test mesotheliomas based on the 27 gene risk classifier. The poor-risk and good-risk groups differ significantly ($P < 0.0001$), but there is no difference in progression times between the gene predicted good-risk group and the actual long-term survivors ($P = 0.8977$), or between the gene predicted poor-risk group and the actual short-term survivor progression times ($P = 0.4799$).

0.034), inflammatory responses ($P = 0.022$), apoptosis induction by extracellular signals ($P = 0.001$), DNA damage response, activation of p53 ($P = 0.001$), and RNA processing ($P = 0.006$). The *P* was calculated using a binomial distribution (21).

Survival and Recurrence Prognostication: Test Set. The dendogram defined by the 27 common genes identified a "poor risk" and "good risk" group of MPMs within this test set ($P = 0.0018$). The median survival of the actual short-term survival group was 3.6 months and that of the predicted poor risk group was 4.3 months (Fig. 4, *A* and *B*). No observed propensity for segregation of epithelial mesotheliomas into the good-risk group or other histologies into the poor-risk group was observed. Time-to-progression curves for the gene set also mirrored the test set actual clinical data (Fig. 4, *C* and *D*).

There were statistical differences in survival ($P = 0.0484$) between actual stage I (median survival not reached), stage II (median survival 10 months), and stage III (median survival 5.2 months) patients (Fig. 5, *A* and *B*). Prognostic heterogeneity, however, was detected within stages when survivals and progression were examined based on the gene classifier. When surgically staged I and II patients were grouped together, their survival was significantly different depending on which cluster the 27 gene classifier assigned them to. As seen in Fig. 5*C*, the patients in either stage 1 or 2 who were assigned to the poor-risk cluster were found to have significantly shorter survival than those assigned to the other cluster ($P = 0.0042$), and the time to progression of the stage I and II patients (Fig. 5*D*) was 1.8 months for those assigned to the poor-risk cluster and 15 months for those in the good-risk cluster ($P = 0.0042$). These differences were only suggestive for the stage III mesothelioma patients with regard to survival (Fig. 5, *E* and *F*). There was, however, a statistically longer time to progression for those stage III mesotheliomas who were clustered as good-risk (17 month median) compared with the poor-risk cluster (2.6 month median; $P = 0.0397$).

Validation with an Independent Set of Pleural Mesotheliomas. We assessed the performance of the 27 gene neural network classifier using oligonucleotide gene expression data obtained from a completely independent [Brigham and Women's (B&W) Hospital] sample of 17 resected MPMs, all stages I or II. First, we trained our neural network with the genes selected by dChip from our dataset, and then the neural network was used to classify patients from B&W dataset. The classification accuracy is only 52.94%. The neural network built with genes selected by SAM from our dataset also did not yield a good result with a classification accuracy of only 47.05%. The classifier built with the common genes between dChip genes and SAM genes yielded a classification accuracy of 76.47% (Table 2), and based on our 27 important

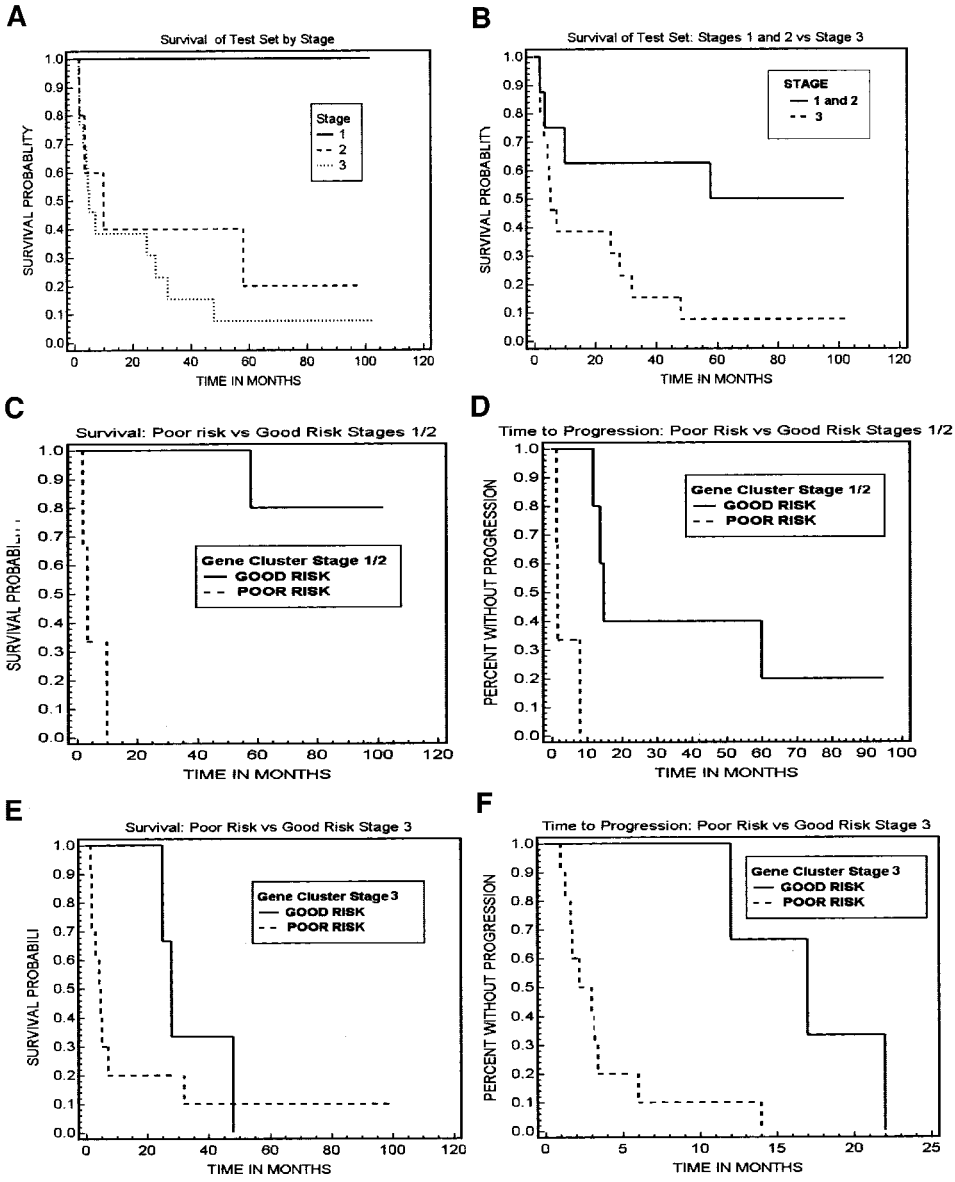

Fig. 5 Gene expression in mesothelioma detects heterogeneity of natural history between patients with similar surgical stages. *A,* actual survival times of the mesothelioma test set by stage at surgery. There were significant differences between the stages. *B,* actual survival times depicted as early disease, *i.e.,* stages 1 and 2 ($n = 8$), compared with late disease, *i.e.,* stage 3 ($n = 13$). Survivals differences were significant ($P = 0.0372$). *C,* staging heterogeneity defined by gene classifier. When the 27 gene classifier was examined in stage 1 and 2 patients, those patients assigned to the good-risk group ($n = 5$) had a significantly longer survival than those assigned to the poor-risk group ($n = 3$; $P = 0.0042$), and the time to progression (*D*) was also significantly longer among stage 1 and 2 patients who were classified as good risk ($P = 0.0042$); *E* and *F,* among stage 3 patients, significant survival differences were not seen between good-risk patients ($n = 3$) and poor-risk patients ($n = 10$; $P = 0.3246$), but significant heterogeneity for time to progression was observed when genetic classification differed ($P = 0.0397$).

genes, we applied hierarchical clustering on the patients from B&W dataset. The resulting dendogram revealed two groups (Fig. 6*A*) from the B&W data, and the predicted survival of the B&W patients (Fig. 6*C*) was similar to their actual (Fig. 6*B*) survival (median survival, 5.5 months *versus* 5 months) for the poor-risk groups. Moreover, the survival differences between the gene-predicted 5 good-risk patients in the B&W and the 12 poor-risk patients approached significance ($P = 0.0511$).

Discussion

Of the 27 genes found to be important in this investigation, 18 have been thoroughly classified in the literature, and few have been associated with MPM. Clusterin SP-40, acidic protein rich in leucine, and cysteine-rich protein were overexpressed in the vast majority of the MPMs, and, hypothetically, could be part of some pathway common to mesothelial carcinogenesis. Selenium binding protein was consistently overexpressed in good-risk patients, and was the only gene common to both the test set and validation set. SIVA or CD27-binding protein is part of an apoptotic pathway induced by CD27 antigen, a member of the tumor necrosis factor receptor superfamily. CD27 regulates the death and differentiation of T and B cells, and provides signals needed for the correct activation of specific T cells. Whether SIVA is important in MPMs for immune surveillance, and as such, could contribute to a longer survival, is unknown. Short chain dehydrogenase/reductase (retSDR1) reduces all-*trans*-retinal during bleached visual pigment regeneration (22). In the absence of retSDR1, and under low concentrations of circulating retinol, the lack of production of vitamin A active

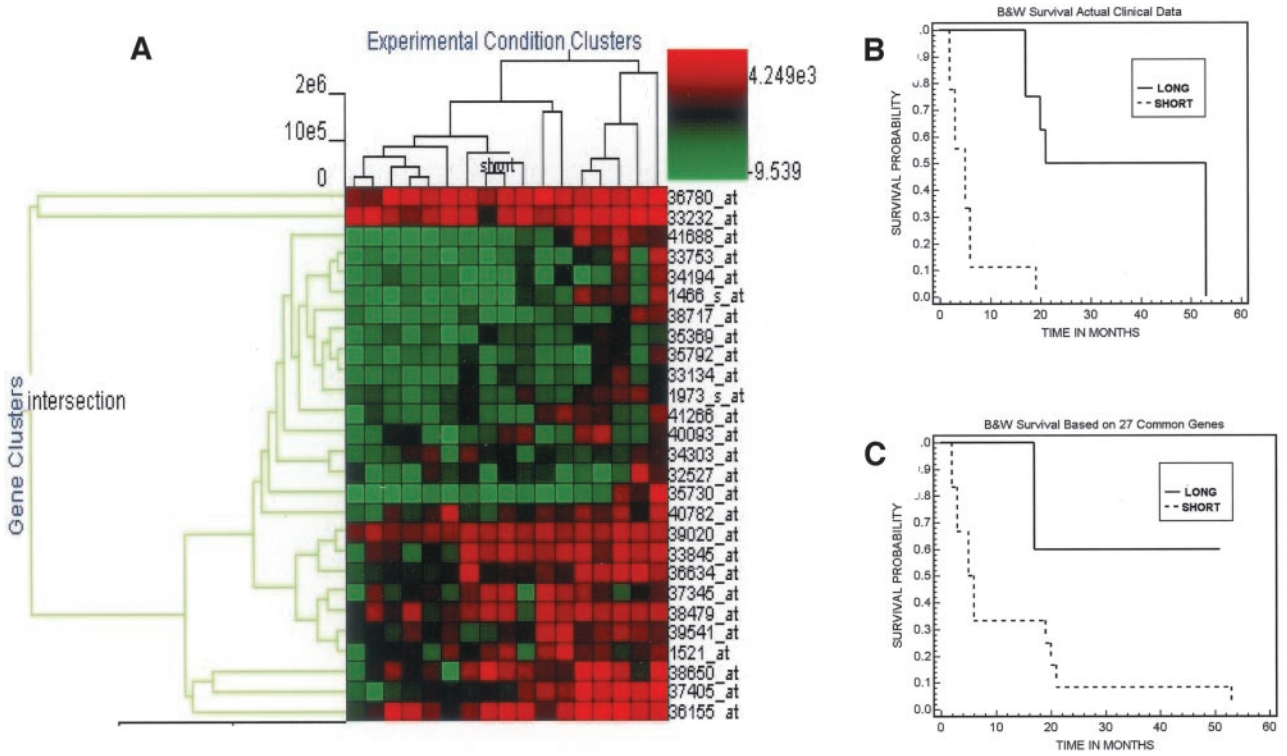

Fig. 6 Validation of gene classifier in other surgically resected mesotheliomas. *A*, gene expression patterns determined using hierarchical clustering of the 17 mesothelioma patients against the 27 common genes between dChip and SAM. Two groups were defined, which have contrasting gene expression patterns similar to that seen in the test set (Fig. 1*B*). *B*, the actual survival time between the short and long term surviving patients in the B&W group was significant ($P = 0.0012$). *C*, the 27 gene classifier defined two groups of mesotheliomas of which the difference in survival approached significance ($P = 0.0511$).

metabolites could contribute to cancer development and progression. Retinoic acid decreases the synthesis of fibronectin and laminin, and migration of MPM implying that retinoids and their binding may decrease MPM local invasion and tumor progression (23). *BTG 2* is a member of a group of structurally related antiproliferative proteins, which mediate a common signal transduction growth arrest and differentiation pathway. This pathway interacts with *N*-methyl transferase, the chief enzyme for post-translational modifications of proteins by protein methylation (24). BTG influences substrates of this methylation pathway including *heterogeneous nuclear ribonucleoproteins (hnRNP*), which was generally lower in expression in the good-risk group. *hnRNP H1* influences pre-mRNA processing, and its role in cancer is unclear; however, *hnRNP H1* has been identified as a protein that binds to the negative regulator spicing element of the Rous Sarcoma Virus (25, 26), and also binds a G-rich element downstream of the core SV40 late polyadenylation signal and stimulates 3′ processing (27). These data suggest that hnRNP H1 could modulate late viral element activity in two known carcinogenic viruses, of which one (SV40) has now been implicated in the pathogenesis of MPM (4).

Calumenin, a calcium binding protein localized in the endoplasmic reticulum involved in protein folding and sorting, was uniformly underexpressed in the good-risk group. Calumenin has been found to bind serum amyloid P (28) and is hypothesized to participate in the immunological defense system. Calumenin has not specifically been associated with MPM before, but serum amyloid A and P have been noted to be connected with MPM (29–31). Nm23a, variably expressed in the good-risk group, was uniformly overexpressed in the poor-risk group. This transcription factor associated with highly metastatic cells (32) plays a role in myc expression. It has been shown that myc can up-regulate nm23-H1 and nm23-H2 expression (33), and data are variable regarding the prognostic significance of nm23 in human neoplasms (34–39).

Our data analysis is novel compared with other reports in the literature. Differences in array platforms, data analysis packages, or modifications in the filtering of the genes may result in differences in classifier genes among reports examining the same disease. We have demonstrated this phenomenon in our own work by comparing the top significant genes of interest from dChip and SAM, and found that there was not uniform agreement between the two programs on these genes, and a 10-fold cross-validation testing yielded differing results for the two programs. We feel that by selecting only those genes that were common to the two analyses, the resulting classifiers are more robust. Moreover, neither the top 27 genes from dChip or SAM could segregate survival differences among the B&W MPMs; however, the common set was 76% accurate in this independent set of specimens. It is likely that the patient population from the National Cancer Institute/Karmanos experience is different from that of the Boston experience. Our group

included patients who were in International Mesothelioma Interest Group stage III, usually on the basis of metastases to the mediastinal lymph nodes at the time of surgery. The Boston MPMs were all stage I or II by the B&W classification, and in this classification, stage II patients may have intraparenchymal lymph node involvement, which would be stage III in the International Mesothelioma Interest Group classification. Moreover, the Boston MPM expression array data would be based on tumors that at the time of surgery did not have disease in the mediastinal lymph nodes (B&W classification stage III). Criteria selection for gene expression differed from the validation set in that the B&W group stipulated minimal expression of 500 and at least 2-fold differences. Given the huge differences in clinical presentation of these subsets, it is actually gratifying that a 76% validation of our gene set could be achieved in the Boston patients.

We have described a set of 27 genes that segregates good-risk and poor-risk surgically treated MPM patients with validation in an independent set of MPM patients. The classifier-predicted good-risk group had significantly longer survival and significantly longer time to progression than the poor-risk group. Moreover, these classifications were independent of the "conventional wisdom" that epithelial mesotheliomas have a better prognosis than biphasic and sarcomatoid histotypes. The data also reflect staging heterogeneity in relation to stage-related prognosis. Good-risk MPMs who were pathological stage I and II had strikingly different survival and time to progression compared with stage I and II patients assigned to the poor-risk cohort. These data reflect the clinical scenario that certain patients with favorable prognostic demographics clinically (*i.e.*, epithelial histology and early stage) nevertheless may recur quickly after operation despite maximal cytoreduction. Such data, after validation in larger numbers of patients, could be important to guide clinical decisions regarding appropriate therapy before committing the MPM patient to surgery.

Acknowledgments

The superb technical assistance of Valerie Murphy, Julia Sluchak-Carlsen, and Apurvi Desai was crucial for the successful completion of these series of studies.

References

1. Zellos, L. S., and Sugarbaker, D. J. Multimodality treatment of diffuse malignant pleural mesothelioma. Semin. Oncol., *29:* 41–50, 2002.

2. La Vecchia, C., Decarli, A., Peto, J., Levi, F., Tomei, F., and Negri, E. An age, period and cohort analysis of pleural cancer mortality in Europe. Eur. J. Cancer Prev., *9:* 179–184, 2000.

3. Manning, C. B., Vallyathan, V., and Mossman, B. T. Diseases caused by asbestos: mechanisms of injury and disease development. Int. Immunopharmacol., *2:* 191–200, 2002.

4. Gazdar, A. F., Butel, J. S., and Carbone, M. SV40 and human tumours: myth, association or causality? Nat. Rev. Cancer, *2:* 957–964, 2002.

5. Liu, Z., and Klominek, J. Regulation of matrix metalloprotease activity in malignant mesothelioma cell lines by growth factors. Thorax, *58:* 198–203, 2003.

6. Ramos-Nino, M. E., Timblin, C. R., and Mossman, B. T. Mesothelial cell transformation requires increased AP-1 binding activity and ERK-dependent Fra-1 expression. Cancer Res., *62:* 6065–6069, 2002.

7. Ohta, Y., Shridhar, V., Bright, R. K., Kalemkerian, G. P., Du, W., Carbone, M., Watanabe, Y., and Pass, H. I. VEGF and VEGF type C play an important role in angiogenesis and lymphangiogenesis in human malignant mesothelioma tumours. Br. J. Cancer, *81:* 54–61, 1999.

8. Foddis, R., De Rienzo, A., Broccoli, D., Bocchetta, M., Stekala, E., Rizzo, P., Tosolini, A., Grobelny, J. V., Jhanwar, S. C., Pass, H. I., Testa, J. R., and Carbone, M. SV40 infection induces telomerase activity in human mesothelial cells. Oncogene, *21:* 1434–1442, 2002.

9. Kumaki, F., Kawai, T., Churg, A., Galateau-Salle, F. B., Hasleton, P., Henderson, D., Roggli, V., Travis, W. D., Cagle, P. T., and Ferrans, V. J. Expression of telomerase reverse transcriptase (TERT) in malignant mesotheliomas. Am. J. Surg. Pathol., *26:* 365–370, 2002.

10. Cacciotti, P., Libener, R., Betta, P., Martini, F., Porta, C., Procopio, A., Strizzi, L., Penengo, L., Tognon, M., Mutti, L., and Gaudino, G. SV40 replication in human mesothelial cells induces HGF/Met receptor activation: a model for viral-related carcinogenesis of human malignant mesothelioma. Proc. Natl. Acad. Sci. USA, *98:* 12032–12037, 2001.

11. Thirkettle, I., Harvey, P., Hasleton, P. S., Ball, R. Y., and Warn, R. M. Immunoreactivity for cadherins, HGF/SF, met, and erbB-2 in pleural malignant mesotheliomas. Histopathology, *36:* 522–528, 2000.

12. Carbone, M., Rizzo, P., Grimley, P. M., Procopio, A., Mew, D. J., Shridhar, V., de Bartolomeis, A., Esposito, V., Giuliano, M. T., Steinberg, S. M., Levine, A. S., Giordano, A., and Pass, H. I. Simian virus-40 large-T antigen binds p53 in human mesotheliomas [see comments]. Nat. Med, *3:* 908–912, 1997.

13. Lew, F., Tsang, P., Holland, J. F., Warner, N., Selikoff, I. J., and Bekesi, J. G. High frequency of immune dysfunctions in asbestos workers and in patients with malignant mesothelioma. J. Clin. Immunol., *6:* 225–233, 1986.

14. Gordon, G. J., Jensen, R. V., Hsiao, L. L., Gullans, S. R., Blumenstock, J. E., Ramaswamy, S., Richards, W. G., Sugarbaker, D. J., and Bueno, R. Translation of microarray data into clinically relevant cancer diagnostic tests using gene expression ratios in lung cancer and mesothelioma. Cancer Res., *62:* 4963–4967, 2002.

15. Rusch, V. W. A proposed new international TNM staging system for malignant pleural mesothelioma. Chest, *108:* 1122–1129, 1995.

16. Gordon G. J., Jensen, R. V., Hsiao, L. L., Gullans, S. R., Blumenstock, J. E., Richards, W. G., Jaklitsch M. T., Sugarbaker, D. J., and Bueno, R. Prediction of outcome in mesothelioma using gene expression ratios. J. Natl. Cancer Inst. (Bethesda), *95:* 598–605, 2003.

17. Khatri, P., Draghici, S., Ostermeier, G. C., and Krawetz, S. A. Profiling gene expression using onto-express. Genomics, *79:* 266–270, 2002.

18. Ashburner, M., Ball, C. A., Blake, J. A., Botstein, D., Butler, H., Cherry, J. M., Davis, A. P., Dolinski, K., Dwight, S. S., Eppig, J. T., Harris, M. A., Hill, D. P., Issel-Tarver, L., Kasarskis, A., Lewis, S., Matese, J. C., Richardson, J. E., Ringwald, M., Rubin, G. M., and Sherlock, G. Gene ontology: tool for the unification of biology. The Gene Ontology Consortium. Nat. Genet., *25:* 25–29, 2000.

19. Li, C., and Wong, W. H. Model-based analysis of oligonucleotide arrays: expression index computation and outlier detection. Proc. Natl. Acad. Sci. USA, *98:* 31–36, 2001.

20. Alizadeh, A. A., Eisen, M. B., Davis, R. E., Ma, C., Lossos, I. S., Rosenwald, A., Boldrick, J. C., Sabet, H., Tran, T., Yu, X., Powell, J. I., Yang, L., Marti, G. E., Moore, T., Hudson, J., Jr., Lu, L., Lewis, D. B., Tibshirani, R., Sherlock, G., Chan, W. C., Greiner, T. C., Weisenburger, D. D., Armitage, J. O., Warnke, R., and Staudt, L. M. Distinct types of diffuse large B-cell lymphoma identified by gene expression profiling. Nature (Lond.), *403:* 503–511, 2000.

21. Draghici, S., Khatri, P., Martins, R., Ostermeier, G. C., and Krawetz, S. A. Global functional profiling of gene expression. Genomics, *81:* 98–104, 2003.

22. Cerignoli, F., Guo, X., Cardinali, B., Rinaldi, C., Casaletto, J., Frati, L., Screpanti, I., Gudas, L. J., Gulino, A., Thiele, C. J., and Giannini, G. retSDR1, a short-chain retinol dehydrogenase/reductase, is retinoic acid-inducible and frequently deleted in human neuroblastoma cell lines. Cancer Res., *62:* 1196–1204, 2002.

23. Scarpa, S., Giuffrida, A., Palumbo, C., Coletti, A., Cerrito, M. G., Vasaturo, F., Sinibaldi, P., Simonelli, L., Procopio, A., and Modesti, A. Retinoic acid inhibits fibronectin and laminin synthesis and cell migration of human pleural mesothelioma in vitro. Oncol. Rep., *9:* 205–209, 2002.

24. Matsuda, S., Rouault, J., Magaud, J., and Berthet, C. In search of a function for the TIS21/PC3/BTG1/TOB family. FEBS Lett., *497:* 67–72, 2001.

25. Fogel, B. L., McNally, L. M., and McNally, M. T. Efficient polyadenylation of Rous sarcoma virus RNA requires the negative regulator of splicing element. Nucleic Acids Res., *30:* 810–817, 2002.

26. Fogel, B. L., and McNally, M. T. A cellular protein, hnRNP H, binds to the negative regulator of splicing element from Rous sarcoma virus. J. Biol. Chem., *275:* 32371–32378, 2000.

27. Bagga, P. S., Arhin, G. K., and Wilusz, J. DSEF-1 is a member of the hnRNP H family of RNA-binding proteins and stimulates pre-mRNA cleavage and polyadenylation in vitro. Nucleic Acids Res., *26:* 5343–5350, 1998.

28. Vorum, H., Jacobsen, C., and Honore, B. Calumenin interacts with serum amyloid P component. FEBS Lett., *465:* 129–134, 2000.

29. Adams, A. L., Castro, C. Y., Singh, S. P., and Moran, C. A. Pleural amyloidosis mimicking mesothelioma: a clinicopathologic study of two cases. Ann. Diagn. Pathol., *5:* 229–232, 2001.

30. Husby, G., Marhaug, G., and Sletten, K. Amyloid A in systemic amyloidosis associated with cancer. Cancer Res., *42:* 1600–1603, 1982.

31. Kayser, K., Ziehms, S., Kayser, G., Andre, S., Bovin, N. V., Dong, X., Kaltner, H., and Gabius, H. J. Glycohistochemical properties of malignancies of lung and pleura. Int. J. Oncol., *12:* 1189–1194, 1998.

32. Roymans, D., Willems, R., Van Blockstaele, D. R., and Slegers, H. Nucleoside diphosphate kinase (NDPK/NM23) and the waltz with multiple partners: possible consequences in tumor metastasis. Clin Exp. Metastasis, *19:* 465–476, 2002.

33. Godfried, M. B., Veenstra, M., Sluis, P., Boon, K., Asperen, R., Hermus, M. C., Schaik, B. D., Voute, T. P., Schwab, M., Versteeg, R., and Caron, H. N. The N-myc and c-myc downstream pathways include the chromosome 17q genes nm23-H1 and nm23-H2. Oncogene, *21:* 2097–2101, 2002.

34. Forte, A., D'Urso, A., Gallinaro, L. S., Lo, S. G., Soda, G., Bosco, D., Bezzi, M., Vietri, F., and Beltrami, V. NM23 expression as prognostic factor in colorectal carcinoma. G. Chir., *23:* 61–63, 2002.

35. Katakura, H., Tanaka, F., Oyanagi, H., Miyahara, R., Yanagihara, K., Otake, Y., and Wada, H. Clinical significance of nm23 expression in resected pathologic-stage I, non-small cell lung cancer. Ann. Thorac. Surg., *73:* 1060–1064, 2002.

36. Martin, K. K., and Pilkington, G. J. Nm23: an invasion suppressor gene in CNS tumours? Anticancer Res., *18:* 919–926, 1998.

37. Tas, F., Tuzlali, S., Aydiner, A., Saip, P., Salihoglu, Y., Iplikci, A., and Topuz, E. Prognostic role of nm23 gene expression in patients with ovarian cancer. Am. J. Clin. Oncol., *25:* 164–167, 2002.

38. Hwang, B. G., Park, I. C., Park, M. J., Moon, N. M., Choi, D. W., Hong, W. S., Lee, S. H., and Hong, S. I. Role of the nm23-H1 gene in the metastasis of gastric cancer. J. Korean Med. Sci., *12:* 514–518, 1997.

39. Nesi, G., Palli, D., Pernice, L. M., Saieva, C., Paglierani, M., Kroning, K. C., Catarzi, S., Rubio, C. A., and Amorosi, A. Expression of nm23 gene in gastric cancer is associated with a poor 5-year survival. Anticancer Res., *21:* 3643–3649, 2001.